Acta Solum 4, Number 1 (November 2025), 13–23.
DOI: 10.20527/actasolum.v4i1.3438
http://jtam.ulm.ac.id/index.php/actasolum
e-ISSN: 2987-5145

USLE-Based Spatial Analysis of Soil Erosion Risk in the Brangkal Sub-Watershed, Mojokerto

Dimas Prabowo Harliando*, Zumrotun Yogi Noviana, Ulfa Rizkika Mufadhila, Dewi Shasa Belia

Department of Agrotechnology, Faculty of Agriculture, Universitas Pembangunan Nasional "Veteran" Jawa Timur, Surabaya, Indonesia

* Correspondence author's email: dimas.prabowo.fp@upnjatim.ac.id

Article Information

Received August 20th 2025
Accepted November 23rd 2025
Published November 30th 2025
Online November 30th 2025

Keywords:

ArcGIS; Brangkal sub-watershed; Soil conservation; Soil erosion; USLE

Abstract

Soil erosion in upland watersheds reduces land productivity, degrades water quality, and threatens ecological services, particularly in areas undergoing tourism-driven land-use change. This study quantified and mapped soil erosion in the Brangkal Sub-Watershed, with a focus on the Pacet Hills tourism area in Mojokerto, East Java. The study employed the Universal Soil Loss Equation (USLE) in combination with ArcGIS, incorporating rainfall erosivity (R), soil erodibility (K), slope length–steepness (LS), land cover (C), and conservation practice (P). Rainfall erosivity was derived from five-year precipitation records using the Lenvain method, soil erodibility from laboratory-analyzed texture and organic matter, LS from a 30 m DEM, and CP from land-use classification adjusted with field observations. All factors were rasterized and multiplied cell-by-cell in ArcGIS to generate annual soil loss estimates and hazard maps. Results indicated annual soil loss between 7.24 and 1922.75 ton ha^{-1} yr^{-1}, with severe erosion concentrated in steep, intensively cultivated upper-catchment zones where LS and CP values are high. Field-derived and reference K values were in close agreement, validating the reliability of hotspot identification. Soils, dominated by Andisols and Inceptisols, exhibited moderate to high erodibility, especially under reduced vegetation cover. Recommended management priorities are vegetative reinforcement, structural slope stabilization, nutrient and pH correction, and land-use zoning to minimize disturbances in high-risk areas. The integration of USLE and GIS provides a robust framework for prioritizing conservation actions that protect soil resources while sustaining the ecological and tourism value of Pacet Hills.

1. Introduction

Soil erosion threatens land productivity, hydrological stability, and ecological resilience, especially in hilly, intensively used landscapes. In regions undergoing rapid land-use changes driven by tourism expansion, such as the upland areas of East Java, Indonesia, the erosion process is often accelerated, resulting in sedimentation, reduced soil fertility, decreased agricultural productivity, and deterioration of downstream water quality (Issaka & Ashraf, 2017; Rashmi et al., 2022).

The Brangkal Sub-Watershed, a tributary within the Brantas River Basin, exemplifies this vulnerability due to its sloping terrain, high rainfall intensity, and expanding human activities (Handayani et al., 2023). Pacet Hills functions as a prominent natural tourism destination, valued for its scenic landscapes, hot springs, and biodiversity area in Pacet District, Mojokerto Regency. These ecosystems moderated hydrological processes, reduced runoff, and protected soil resources. However, shifts in land use following the decline of tourism activity, including the expansion of cultivation on steep slopes and the conversion of open spaces into settlement have altered vegetation cover and increased the vulnerability of soils to detachment and transport.

Despite the ecological significance of the area, data on the spatial distribution and severity of erosion remain limited. Addressing this gap requires an integrated geospatial approach capable of capturing the complex interactions between topography, land use, and soil properties. ArcGIS, as a powerful spatial analysis tool, enables precise mapping and assessment of erosion-prone zones by processing multi-layered environmental datasets (J. Wang et al., 2024).

This study contributes novelty by explicitly linking soil erosion risk assessment with tourism-driven land-use change in a highland watershed. While previous research has applied USLE and GIS for agricultural or forestry contexts, few studies have examined how erosion hotspots intersect with ecotourism landscapes where land productivity, ecological integrity, and tourism value are simultaneously at stake. By integrating biophysical erosion modeling with land-use zoning considerations, this research provides a framework for sustainable land management that balances conservation priorities with tourism development

2. Material and Methods

2.1. Study Area

This study was conducted within the Brangkal Sub-Watershed covers an area of about 103.8 ha (1.04 km²), forming part of the upper Brantas River Basin located in East Java Province, Indonesia. The focal site is the De Picnic tourism area, situated in Pacet District, Mojokerto Regency, positioned at approximately coordinates 7°41′5.6"S, 112°33′32.65"E. The area exhibits hilly terrain with moderate to steep slopes. Climatically, it receives an average annual rainfall of ~3,600 mm, with 4–8 wet months per year (Oldeman Type C climate), and mean annual temperature ranges between 22–24 °C, receiving substantial rainfall throughout the year, making it vulnerable to surface erosion. The site is bounded by Kutorejo District (north), Gondang (west), Trawas District (east), and forestmixed-agriculture zones (south). These adjacent land uses influence runoff behavior and erosion dynamics in the Brangkal Sub-Watershed catchment.

2.2. Data Analysis

The spatial analysis of soil erosion employed the Universal Soil Loss Equation (USLE) integrated with ArcGIS in a raster-based approach. Each factor, rainfall erosivity (R), soil erodibility (K), slope length and steepness (LS), land cover (C), and conservation practices (P), was converted into a geospatial layer. All layers were standardized to a uniform spatial resolution. Rainfall erosivity was derived from NASA precipitation datasets spanning the last five years, aggregated and processed using the Lenvain method (Banuwa,M.Si, 2013) to produce a climatological R-factor layer. The Lenvain method estimates erosivity based on monthly rainfall totals, where higher rainfall amounts are weighted more heavily to reflect their greater potential to detach and transport soil particles. This empirical approach has been widely applied in Indonesia as a practical alternative to event-based erosivity calculations, which require high-resolution rainfall intensity data that are often unavailable. Soil erodibility values were computed following (Wischmeier et al., 1971) using texture and permeability attributes, then rasterized for overlay.

$$100\,K = 1.292\,[2.1 \times 10^{-4} \times \left((12 - OM)M^{1.14}\right) + 3.25(S-2) + 2.5(P-3)]$$

Where K is the soil erodibility factor, OM is the organic matter content (%), M is the soil texture factor calculated as (% silt + % very fine sand) × (100 – % clay), s is the soil structure code, and P is the soil permeability class
The LS factor was computed from slope gradients derived from a hydrologically corrected Digital Elevation Model (DEM) with 8 m resolution, resampled to 30 m to match other datasets. Information on land use and vegetation cover from the Mojokerto region was reclassified into C and P factors based on literature coefficients adapted to local conditions and adjusted with field observations. For example, dry forest = 0.001, paddy field = 0.02, cultivated fields = 0.19, bushland = 0.10. The full coefficient table is provided (Table 4) to ensure reproducibility. Vector land-use data were converted to raster format using the nearest-neighbor assignment method to preserve the categorical integrity of land-cover classes. All rasters were multiplied cell-by-cell to compute the yearly soil erosion rate (A) measured in metric tons per hectare. The resulting erosion hazard map was classified into five categories: very low, low, moderate, high, and very high to interpret the spatial risk profile. The equation used to calculate the erosion hazard level is as follows (Wischmeier & Smith, 1978):

A = R*K*LS*CP

Where A is annual erosion (ton ha^{-1} $year^{-1}$), R is rainfall erosivity index (MJ mm ha^{-1} h^{-1} yr^{-1}). K is soil erodibility index (ton h MJ^{-1} mm^{-1}), LS is slope length and steepness index, CP is land cover and conservation practices index All USLE factors were expressed in standard international units following USDA (Wischmeier & Smith, 1978) and FAO guidelines to ensure consistency.

3. Results and Discussion

3.1. Rainfall Erosivity Parameter (R)

The analysis of the Rainfall Erosivity Index (R-factor) reveals spatial variations in erosive potential across the study area. Using historical rainfall data and applying the standardized formula for R-factor calculation, we generated a comprehensive erosivity map that visualizes the intensity and distribution of rainfall-induced erosion risk in Figure 1.

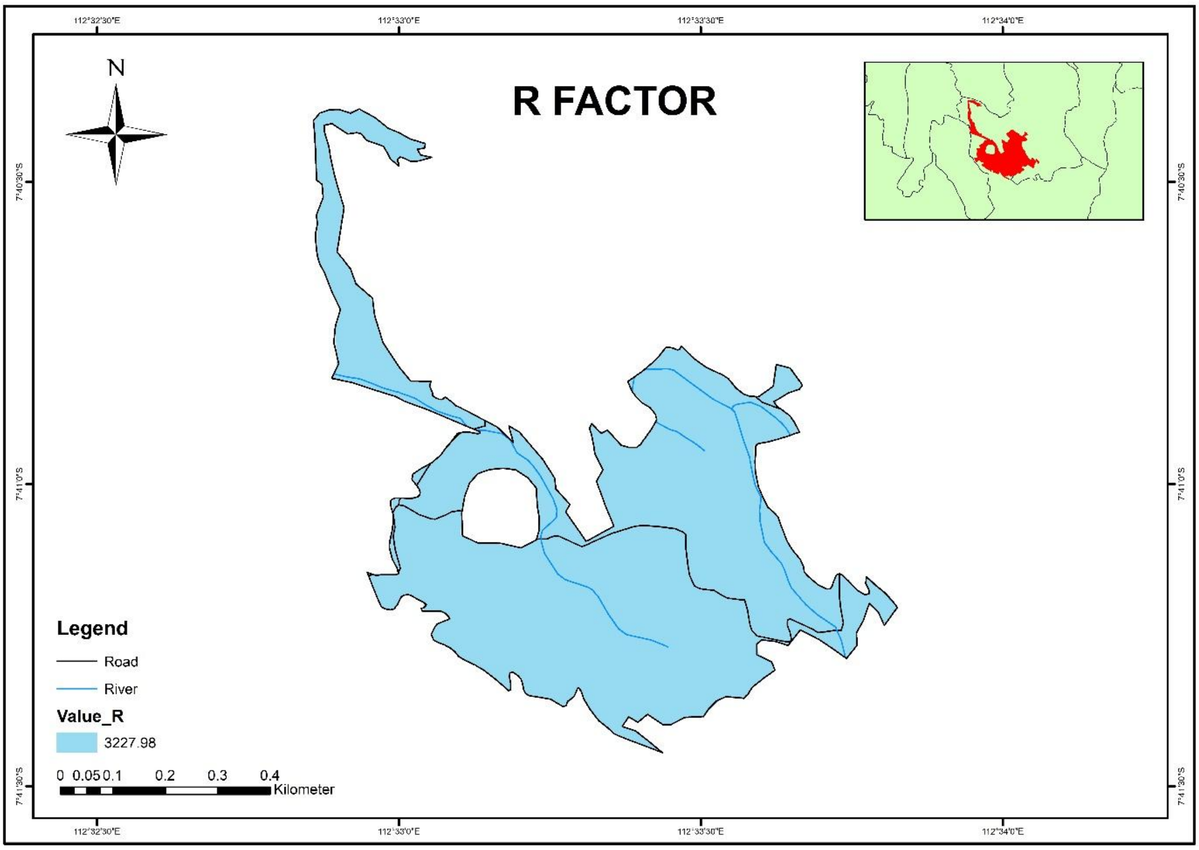

Figure 1. Rainfall erosivity (R-factor) map of the Pacet Hills area, Brangkal Sub-Watershed

The calculated rainfall erosivity (R) factor for the Brangkal Sub Watershed is 3227.98 MJ·mm·ha^{-1}·h^{-1}·yr^{-1}, with a uniform value across the study area. This homogeneity reflects two key aspects: the relatively small spatial extent of the watershed 103.8 ha, which lies within a single, consistent topoclimatic zone, and the use of rainfall data from a single representative station, eliminating spatial interpolation between multiple gauges. According to the Oldeman rainfall classification, the study area experiences approximately four to eight wet months annually (Table 1), each with monthly rainfall exceeding 200 mm. This places the Brangkal Sub-Watershed in a Type C climate zone, which is characterized by moderate wetness and typically supports seasonal cropping systems. Such conditions reinforce the area's susceptibility to rainfall-induced soil erosion, each with monthly rainfall exceeding 200 mm, reinforcing its susceptibility to rainfall-induced soil erosion.

Rainfall totals (mm) for 2020–2024. The R-factor was calculated using the Lenvain method ($R = 2.21P^{1.36}$, where P is monthly rainfall), resulting in a watershed erosivity index of 3227.98 MJ·mm·ha^{-1}·h^{-1}·yr^{-1}. Rainfall erosivity describes the capacity of precipitation to induce soil erosion, measuring both the energy and intensity of rainfall events that detach and move soil particles (Nearing et al., 2017). The magnitude of rainfall erosivity is influenced by multiple factors, including high rainfall intensity, raindrop size, and precipitation duration (Almeida et al., 2021). These variables collectively enhance the kinetic energy imparted by rainfall, thereby accelerating the disintegration of the soil surface and consequently increasing the rate of erosion. Recent research underscores that areas surrounding Mojokerto Regency experience rainfall conditions with the potential to generate moderate to high erosivity, particularly in areas with steep slopes and inadequate vegetative cover. Similar rainfall patterns with high erosivity have been reported in Pasuruan (Hidayat et al., 2020), while vegetation indices were shown to influence rainfall intensity in East Java (Suharyanto et al., 2024).

Table 1. Rainfall data for the Pacet Hills area study 2020 - 2024

Rainfall	**Year**				
	2020	**2021**	**2022**	**2023**	**2024**
Jan	387	761.1	693.1	334.9	412.2
Feb	817.5	723.3	268.4	754.3	454
Mar	638.3	996	478.2	260	487.3
Apr	370.7	259.1	484.3	754.5	470.9
Mei	352	195.1	359.7	118.7	20.2
Jun	16.9	323	155.5	17.3	104.1
Jul	35.9	200	28	14	38
Aug	72.7	100	92.5	0	213
Sept	0	44.4	36	3.2	63.8
Oct	67.3	276.3	343.4	0	35.4
Nov	363.7	442.8	400.8	109.4	173.8
Dec	619.8	390.1	419.7	68.3	944.5
Total	3741.8	4711.2	3759.6	2434.6	3417.2

3.2. Soil Erodibility Parameter (K)

Soil erodibility is a measure of how easily soil particles can be detached and transported by erosive forces such as rainfall, surface runoff (Renard et al., 1997; B. Wang et al., 2013). The spatial distribution map of the K-factor is presented in Figure 2, illustrating variations in soil erodibility across the study area.

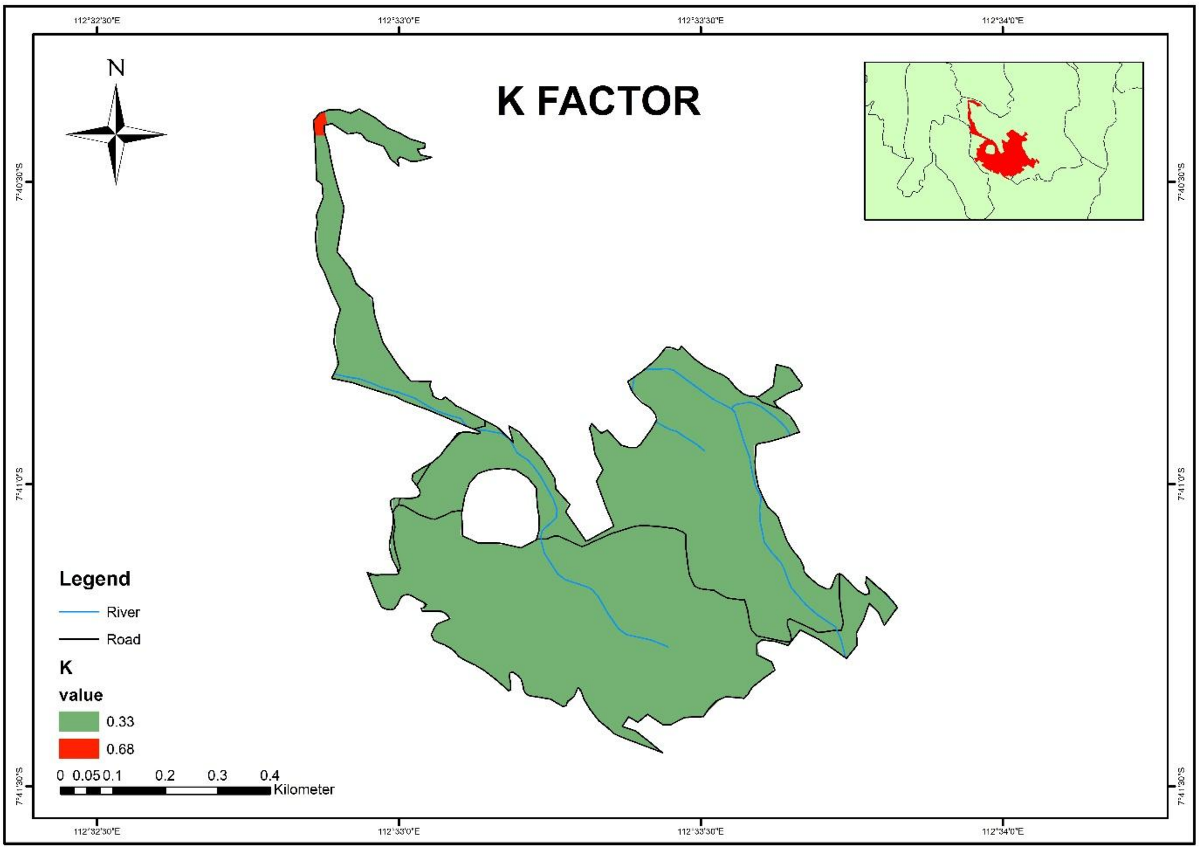

Figure 2. Soil erodibility (K-factor) map of the Pacet Hills area, Brangkal Sub-Watershed

Soil erodibility depends on a combination of natural soil traits, including particle size distribution, structural arrangement, organic content, and infiltration capacity (Shafii et al., 2023). Soils characterized by a fine texture, particularly with substantial silt proportions, are more susceptible to detachment due to their low cohesion, whereas well-developed granular structures enhance aggregate stability and resistance to erosion (Yuan & Fan, 2024). Higher organic matter content contributes to particle binding and improved structural integrity, thereby reducing erodibility (Guo et al., 2024; Smith et al., 2022). Conversely, soils with low permeability generate greater surface runoff, increasing the potential for particle transport under erosive forces (G. Wang et al., 2015).

The latest research in Mojokerto Regency indicates considerable spatial variability in soil erodibility, driven by differences in land use, slope, and intrinsic soil properties. The principal soil categories present within the study site are Andisols and Inceptisols. Andisols, derived from volcanic ash, are typically rich in organic matter, have low bulk density, and exhibit well-developed aggregate stability structure, maintained by short-range-order minerals, such as allophane and imogolite (Arnalds, 2015). These characteristics promote high infiltration and aggregate stability, which can lower erodibility, though the low bulk density can make surface horizons more prone to detachment under intense rainfall if vegetation cover is lacking. Inceptisols, in contrast, are weakly developed soils with moderate weathering, variable textures (ranging from sandy loam to clay), and generally lower organic matter content (Soil Staff Survey, 2022). Their less stable aggregates and, in some cases, finer textures can promote surface sealing and runoff, resulting in relatively higher erodibility compared with Andisols under similar land-cover conditions.

The K-factor in this study was calculated using particle-size distribution, organic matter content, soil structure, and permeability, with results shown in Table 2. For comparison, reference K-values based on soil type classification were also incorporated to verify consistency between field-derived estimates and established empirical parameters, thereby enhancing the robustness of the erosion potential assessment.

Table 2. K Index of Study Area

Soil Type	K Index (Actual)	K Index (Reference)
Andisol	0.33	0.28
Inceptisol	0.68	0.39

3.3. Slope Gradient and Length Parameter (LS)

The Slope Gradient and Length Parameter LS-factor) is a key topographic parameter in soil erosion models such as the Universal Soil Loss Equation (USLE) and its revised form (RUSLE), representing the combined effect of slope length and slope gradient on erosion potential (Das et al., 2022; Yang, 2015). - The slope length component (L-factor) denotes the horizontal distance from the starting point of surface runoff to the location where the flow decelerates enough for deposition or enters a defined channel (Lu et al., 2020). The slope steepness term (S-factor) represents the effect of gradient, with steeper slopes accelerating runoff and enhancing runoff velocity, and promoting greater soil particle detachment and transport (Deng et al., 2020). The spatial distribution of the LS index is illustrated in Figure 3.

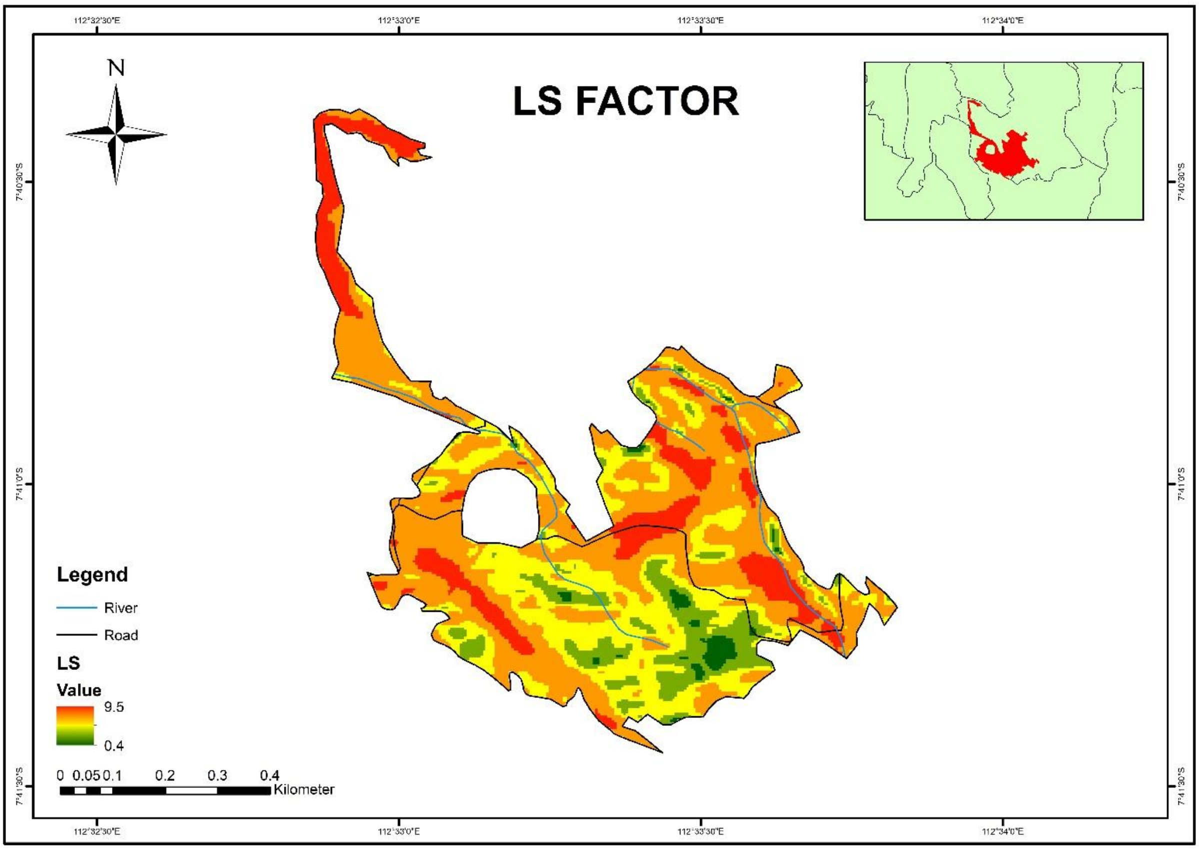

Figure 3. Slope gradient and length (LS-factor) map of the Pacet Hills area, Brangkal Sub-Watershed

The determination of the LS (length–slope) factor is based on the combination of slope length and slope steepness, as classified in Table 3. Within the Pacet Hills Sub-Watershed, the topography is predominantly characterised by slopes of 15–45%, representing moderately steep to steep classes in standard landform classifications.

Table 3. Relationship between slope gradient and LS

Slope Class	Slope Gradient	LS
I	0 -8 %	0,4
II	8 – 15 %	1,4
III	15 – 25 %	3,1
IV	25 – 40 %	6,8
V	> 40 %	9,5

Across the watershed, LS values are relatively high, often exceeding 6.0 in upper catchment ridges and elongated slopes, where steep gradients and long slopes amplify runoff velocity and erosive power. This topographic configuration substantially elevates the potential for soil detachment and transport, particularly where protective vegetation cover is sparse or where land use involves intensive cultivation along the slope gradient.

3.4. Land Cover and Soil Conservation Parameter (CP)

The Land Cover and Soil Conservation Parameter (CP) index in the USLE framework represents the overall influence exerted by cropping patterns, vegetation cover, and conservation measures on soil erosion rates (Xiong et al., 2023). The CP values were derived by relating land use types to established reference values, and the geographic distribution of the CP index is presented in Figure 4.

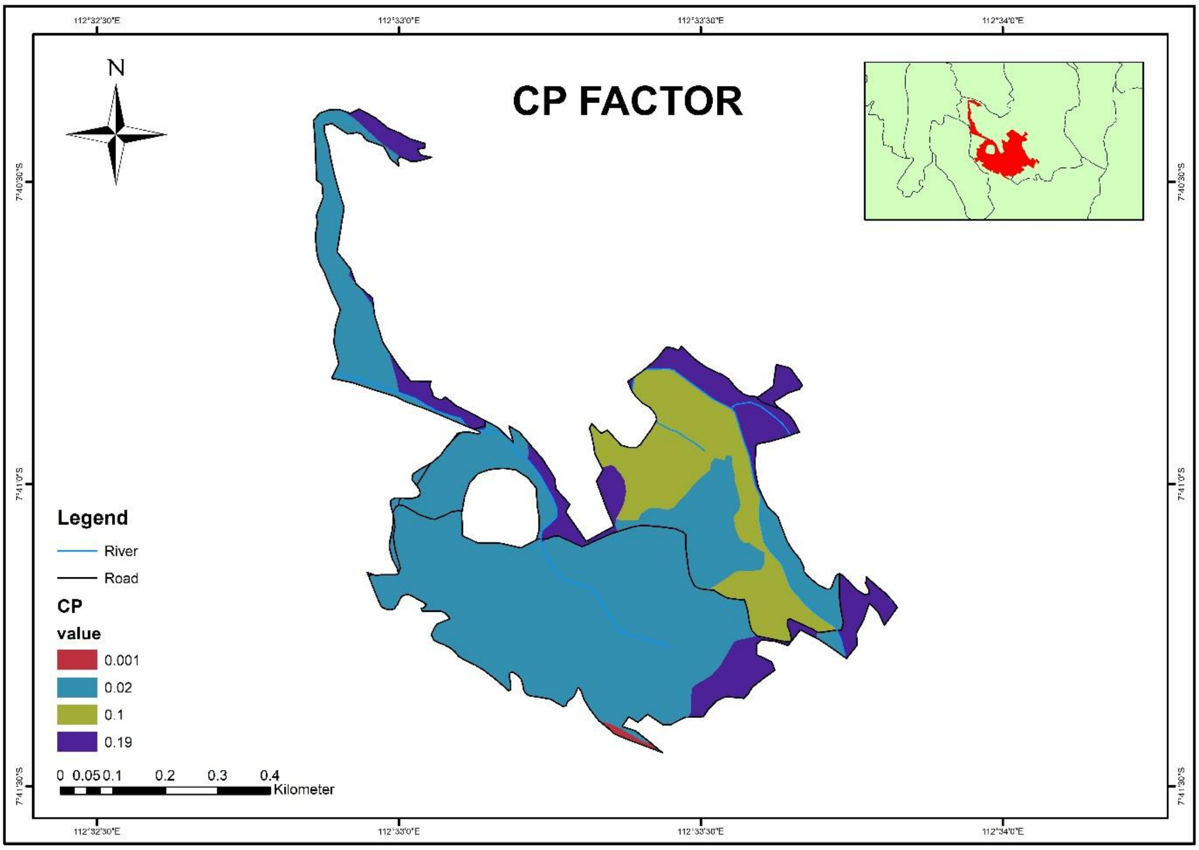

Figure 4. Land cover and soil management (CP-factor) map of the Pacet Hills area, Brangkal Sub-Watershed

The CP value essentially reflects how differences in land use, such as forests, built-up areas, grasslands, plantations, or bare land, and land management practices, including the application of terracing, mulching, contour farming, and others, can mitigate the kinetic energy effect of precipitation and overland flow that may erode the soil surface (Desta et al., 2021). A low CP value indicates that the land use and management in the area provide good protection for the soil, whereas a high value suggests the opposite. Within the study area, multiple land-use categories are present, namely dry forest, garden, field, rice field, and bush. For each category, the CP values were determined by referencing the established coefficients in Table 4.

Table 4. Land Cover and Crop Practices (CP) Values in Indonesia

Type of Land Use	CP value
Dry Forest	0.001
Garden	0.02
Field	0.19
Paddy Rice Field	0.02
Bush	0.1

Dry forest (CP = 0.001) provides near-complete protection against soil loss, as dense canopy and litter cover effectively intercept rainfall and reduce runoff energy. In contrast, cultivated fields (CP = 0.19) and bushland (CP = 0.10) contribute substantially higher erosion risk, reflecting the reduced ground cover and weaker capacity to buffer raindrop impact and surface flow

3.5. Soil Erosion

In this study, soil erosion was calculated using two types of K-factor values: the K value obtained directly from field-collected soil samples, and a reference K value used for comparison to evaluate differences in erosion potential. The USLE analysis estimated annual soil erosion in Brangkal Sub-Watershed ranging from 7.24 to

1922.746 ton ha⁻¹ yr⁻¹, with a mean of 617.61 ton ha⁻¹ yr⁻¹. The maximum estimated soil loss (1,922.75 ton ha⁻¹ yr⁻¹) far exceeds the tolerable soil loss threshold in Indonesia (15–50 ton ha⁻¹ yr⁻¹; Arsyad, 2010). Such values are considered catastrophic, indicating that without intervention, soil productivity and watershed stability will be severely compromised. Classification based on the Ministry of Forestry erosion hazard standards indicated that 9.8 % of the area falls under the very low and low hazard category (Table 5), 50,5 % into moderate, and 41,03 % into high to very high categories. Spatially, severe erosion risk is concentrated in the upper catchment (Figure 5), particularly on long, steep slopes dominated by annual crops and thin grass, where LS-factor values exceed the threshold and CP values are relatively high. Analysis using the reference K value indicated that 29.9% of the watershed area fell into low and very low erosion hazard classes, 39.5% into the moderate class, and 30.6% into high and very high classes. The spatial distribution of these hazards was concentrated primarily in the upper watershed zones, coinciding with the critical erosion-prone areas delineated in the actual K value map (Figure 6). While moderate erosion hazard dominates across the Brangkal Sub-Watershed, localized hotspots on steep slopes exhibit accelerated soil loss due to gravitational forces, intense surface runoff, and insufficient protective ground cover.

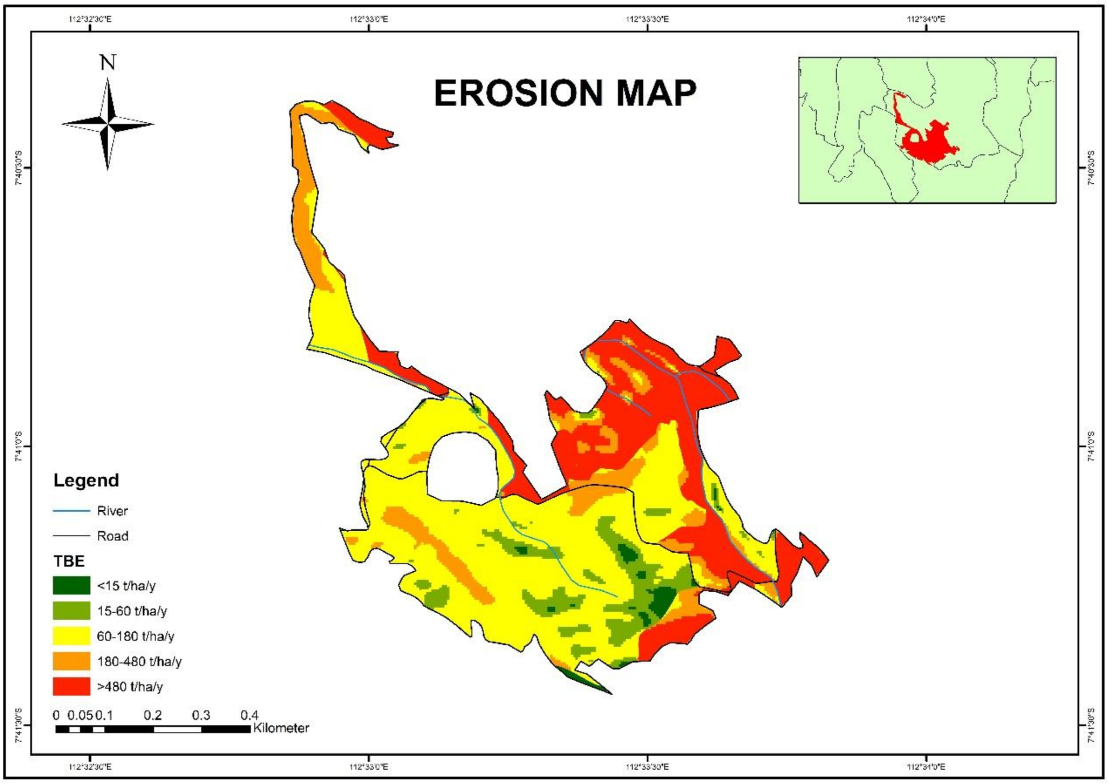

Figure 5. Erosion map in Pacet Hills area using K actual

Areas with low erosion potential are typically located on flatter terrain with perennial vegetation or forest cover, where low CP values and dense canopy effectively dissipate rainfall kinetic energy and reduce surface runoff velocity. Conversely, high rainfall erosivity during peak wet season months amplifies erosion in exposed areas, particularly where soils possess moderate to high K factor values linked to silt-rich textures and weak structural stability. These patterns are consistent with documented findings in the Welang and Parangan watersheds, where similar topographic and land-use configurations have produced erosion rates exceeding 40 ton ha⁻¹ yr⁻¹ in vulnerable zones (Almadilla Setya Putri et al., 2025; Maroeto & Santoso, 2023).

The convergence of steep slopes, intensive cultivation without adequate conservation practices, and high rainfall erosivity underscores the urgent need for targeted soil conservation (Aditya et al., 2024). For high-risk zones such as Pacet Hills an ecotourism asset whose scenic and ecological integrity is central to its economic value sustainable development must integrate vegetative reinforcement through deep-rooted, canopy-forming species to intercept rainfall and reduce detachment forces, structural measures such as contour bunding, terracing, and bioengineering to slow runoff and stabilize slopes, Land-use zoning that restricts high-impact activities on severe slopes to preserve both soil stability and tourism appeal. These recommendations align with best practices (Harliando et al., 2023; Nyairo, 2024; Uniyal et al., 2020) for combining vegetative measures like cover cropping and mulching with engineered interventions (Dibaba et al., 2021). Mapping and quantifying erosion distribution not only provides a benchmark for long-term monitoring but also establishes a prioritization framework for intervention planning, ensuring that conservation investments are directed where they will yield the highest reduction in soil loss.

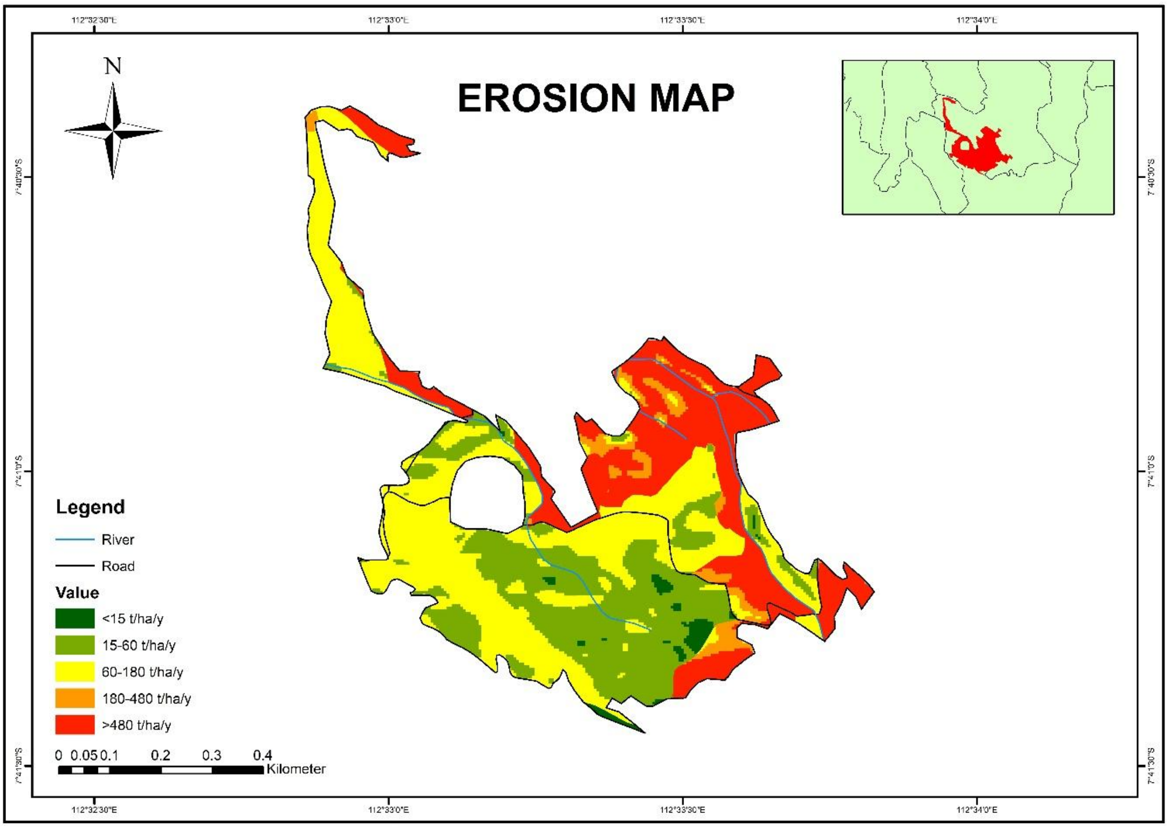

Figure 6. Erosion map in Pacet Hills area using K reference

Table 5. Soil Erosion in Brangkal Sub-Watershed

Erosion rate (ton ha^{-1} $year^{-1}$)	Erosion Class	Percentage (%) K Actual	Percentage (%) K Reference
0–15	Very low	1.6	1.6
15–60	Low	8.2	28.3
60–180	Moderate	50.5	39.5
180–480	High	13.3	4.2
>480	Very high	26.4	26.4

Among the USLE factors, slope length–steepness (LS) emerged as the dominant driver of erosion risk in Pacet Hills, as steep slopes consistently coincided with high erosion classes. Soil erodibility (K) also contributed substantially, particularly in Inceptisols with weak aggregate stability. In contrast, rainfall erosivity (R) was relatively uniform across the watershed, indicating that spatial variability in erosion was controlled more by topography and land cover than by rainfall. The cover–management and conservation practice (CP) factor further amplified soil loss in cultivated areas lacking adequate protection. Together, these results highlight slope steepness and land management as the most critical determinants of erosion in the Brangkal Sub-Watershed.

Importantly, the choice of method for deriving the K factor significantly influences erosion hazard classification. Alternative formulations of K, such as those based on Wischmeier–Smith, EPIC, or WEPP approaches, can yield different magnitudes of erodibility for the same soil type, thereby shifting areas between moderate, high, and very high hazard classes. This methodological sensitivity underscores the need for transparent reporting of K derivation and careful consideration when comparing results across studies.

4. Conclusion

The Brangkal Sub-Watershed exhibits moderate to very high soil erosion risk, with critical hotspots located on steep slopes under intensive cultivation and minimal conservation measures. High rainfall erosivity, elevated LS values, and vulnerable soil properties, particularly in Inceptisol-dominated areas accelerate soil loss and threaten long-term land productivity and watershed stability. Integrating USLE-based spatial analysis with targeted management strategies enables precise identification of priority zones for intervention. Conservation planning should emphasize slope stabilization through terracing, contour farming, and strict land-use zoning to limit cultivation on steep slopes, while also integrating vegetative reinforcement using deep-rooted species such as vetiver grass (Chrysopogon zizanioides) and bamboo (Gigantochloa apus) to stabilize slopes, alongside canopy-forming trees like sengon (Falcataria moluccana) and mahogany (Swietenia macrophylla) to intercept rainfall and reduce detachment forces. These species, combined with contour hedgerows, agroforestry, cover cropping, and complementary measures such as nutrient and pH management, provide site-appropriate protection for Pacet Hills. Implementing these measures will protect both the ecological integrity and the economic value of the Pacet Hills tourism area.

Acknowledgement

The authors gratefully acknowledge the Faculty of Agriculture at Universitas Pembangunan Nasional "Veteran" Jawa Timur for providing laboratory facilities and logistical support throughout this research. We extend our thanks to the Soil Resource Laboratory team for their assistance with sample preparation and analytical procedures.

References

Aditya, H. F., Yuhdistira, M. F., Sholikah, D. H., Harliando, D. P., & Wijayanti, F. 2024. Analisis Erosi Aktual Menggunakan Software ArcGIS pada Sub DAS Durensewu, Waduk Gadjah Mungkur Wonogiri. *G-Tech: Jurnal Teknologi Terapan*, *8*(4), 2744–2754. https://doi.org/10.70609/gtech.v8i4.5358

Almadilla Setya Putri, J., Ussy Andawayanti, & Ery Suhartanto. 2025. Pengendalian Erosi dan Sedimen Berbasis SIG dengan Perencanaan Check Dam di DAS Parangan Kabupaten Pasuruan. *Jurnal Teknologi Dan Rekayasa Sumber Daya Air*, *5*(2), 1043–1052. https://doi.org/10.21776/ub.jtresda.2025.005.02.099

Almeida, W. S. D., Seitz, S., Oliveira, L. F. C. D., & Carvalho, D. F. D. 2021. Duration and intensity of rainfall events with the same erosivity change sediment yield and runoff rates. *International Soil and Water Conservation Research*, *9*(1), 69–75. https://doi.org/10.1016/j.iswcr.2020.10.004

Arnalds, O. 2015. Classification and the Main Soil Types. In O. Arnalds, *The Soils of Iceland* (pp. 55–70). Springer Netherlands. https://doi.org/10.1007/978-94-017-9621-7_6

Arsyad, S. 2010. *Konservasi Tanah dan Air*. Edisi Kedua. IPB Press. Bogor. 472 hal. Retrieved from https://repository.ipb.ac.id/handle/123456789/42667Banuwa, M.Si, P. D. I. I. S. (2013). *Erosi*. Prenada Media. Retrieved from https://books.google.co.id/books?id=fFFADwAAQBAJ&printsec=frontcover&source=gbs_ge_summary_r&cad=0#v=onepage&q&f=false

Das, S., Bora, P. K., & Das, R. 2022. Estimation of slope length gradient (LS) factor for the sub-watershed areas of Juri River in Tripura. *Modeling Earth Systems and Environment*, *8*(1), 1171–1177. https://doi.org/10.1007/s40808-021-01153-0

Deng, L., Sun, T., Fei, K., Zhang, L., Fan, X., Wu, Y., & Ni, L. 2020. Effects of erosion degree, rainfall intensity and slope gradient on runoff and sediment yield for the bare soils from the weathered granite slopes of SE China. *Geomorphology*, *352*, 106997. https://doi.org/10.1016/j.geomorph.2019.106997

Desta, G., Tamene, L., Abera, W., Amede, T., & Whitbread, A. 2021. Effects of land management practices and land cover types on soil loss and crop productivity in Ethiopia: A review. *International Soil and Water Conservation Research*, *9*(4), 544–554. https://doi.org/10.1016/j.iswcr.2021.04.008

Dibaba, W. T., Demissie, T. A., & Miegel, K. 2021. Prioritization of Sub-Watersheds to Sediment Yield and Evaluation of Best Management Practices in Highland Ethiopia, Finchaa Catchment. *Land*, *10*(6), 650. https://doi.org/10.3390/land10060650

Guo, G., Kong, Y., Xu, Y., Peng, X., Niu, M., Zeng, G., Ouyang, Z., Liu, J., Zhang, C., & Lin, J. 2024. Soil organic matter components and sesquioxides integrally regulate aggregate stability and size distribution under erosion and deposition conditions in southern China. *Journal of Hydrology*, *639*, 131588. https://doi.org/10.1016/j.jhydrol.2024.131588

Handayani, D. A., Kurniadi, A., & Bahar, F. 2023. Upstream Brantas Watershed management strategies for flood mitigation (a review: Batu District). *IOP Conference Series: Earth and Environmental Science*, *1173*(1), 012053. https://doi.org/10.1088/1755-1315/1173/1/012053

Harliando, D. P., Setyawan, C., & Mawandha, H. G. 2023. Spatial Modeling of Vegetation Cover for Soil Erosion Control Based on Arc GIS and the RUSLE Models. *Jurnal Teknik Pertanian Lampung (Journal of Agricultural Engineering)*, *12*(1), 14. https://doi.org/10.23960/jtep-l.v12i1.14-27

Hidayat, M. D. N., Indarto, I., Askin, M., Andriyani, I., & Tasliman, T. 2020. Kecenderungan Hujan Ekstrem di Unit Pelaksana Teknis Pengelolaan Sumberdaya Air di Pasuruan, Jawa Timur. *Jurnal Tanah dan Iklim*, *43*(1), 21. https://doi.org/10.21082/jti.v43n1.2019.21-31

Issaka, S., & Ashraf, M. A. 2017. Impact of soil erosion and degradation on water quality: A review. *Geology, Ecology, and Landscapes*, *1*(1), 1–11. https://doi.org/10.1080/24749508.2017.1301053

Lu, S., Liu, B., Hu, Y., Fu, S., Cao, Q., Shi, Y., & Huang, T. 2020. Soil erosion topographic factor (LS): Accuracy calculated from different data sources. *CATENA*, *187*, 104334. https://doi.org/10.1016/j.catena.2019.104334

Maroeto, M., & Santoso, W. 2023. *GIS-based spatial evaluation for land suitability in various land uses in critical land Welang Watershed, Indonesia*. 020066. https://doi.org/10.1063/5.0154804

Nearing, M. A., Yin, S., Borrelli, P., & Polyakov, V. O. 2017. Rainfall erosivity: An historical review. *CATENA*, *157*, 357–362. https://doi.org/10.1016/j.catena.2017.06.004

Nyairo, R. 2024. Effect of slope on water run-off and soil vulnerability in an unglaciated sub-watershed: A case study of conservation practice siting. *Environmental Systems Research*, *13*(1), 50. https://doi.org/10.1186/s40068-024-00380-5

Rashmi, I., Karthika, K. S., Roy, T., Shinoji, K. C., Kumawat, A., Kala, S., & Pal, R. 2022. Soil Erosion and Sediments: A Source of Contamination and Impact on Agriculture Productivity. In M. Naeem, J. F. J. Bremont, A. A. Ansari, & S. S. Gill (Eds.), *Agrochemicals in Soil and Environment* (pp. 313–345). Springer Nature Singapore. https://doi.org/10.1007/978-981-16-9310-6_14

Renard, K. G., USA, & USA (Eds.). 1997. *Predicting soil erosion by water: A guide to conservation planning with the revised universal soil loss equation (RUSLE)*. Retrieved from https://www.tucson.ars.ag.gov/unit/publications/PDFfiles/717.pdf\Shafii, I., Medina-Cetina, Z., Shidlovskaya, A., & Briaud, J.-L. 2023. Relationship between Soil Erodibility and Soil Properties. *Journal of Geotechnical and Geoenvironmental Engineering*, *149*(1), 04022121. https://doi.org/10.1061/(ASCE)GT.1943-5606.0002915

Smith, D. J., Snead, M., & Thompson, T. M. 2022. Soil Amended With Organic Matter Increases Fluvial Erosion Resistance of Cohesive Streambank Soil. *Journal of Geophysical Research: Biogeosciences*, *127*(6), e2021JG006723. https://doi.org/10.1029/2021JG006723

Soil Staff Survey. 2022. Keys to Soil Taxonomy, 13th Edition. *USDA Natural Resources Conservation Service*. Retrieved from https://www.nrcs.usda.gov/sites/default/files/2022-09/Keys-to-Soil-Taxonomy.pdf

Suharyanto, A., Pujiraharjo, A., & Iqbal, M. T. 2024. Influence of vegetation index to the rainfall intensity in Pasuruan Area, East Java Province, Indonesia. *Journal of Applied and Natural Science*, *16*(1), 251–262. https://doi.org/10.31018/jans.v16i1.5316

Uniyal, B., Jha, M. K., Verma, A. K., & Anebagilu, P. K. 2020. Identification of critical areas and evaluation of best management practices using SWAT for sustainable watershed management. *Science of The Total Environment*, *744*, 140737. https://doi.org/10.1016/j.scitotenv.2020.140737

Wang, B., Zheng, F., Römkens, M. J. M., & Darboux, F. 2013. Soil erodibility for water erosion: A perspective and Chinese experiences. *Geomorphology*, *187*, 1–10. https://doi.org/10.1016/j.geomorph.2013.01.018

Wang, G., Fang, Q., Wu, B., Yang, H., & Xu, Z. 2015. Relationship between soil erodibility and modeled infiltration rate in different soils. *Journal of Hydrology*, *528*, 408–418. https://doi.org/10.1016/j.jhydrol.2015.06.044

Wang, J., Yang, J., Li, Z., Ke, L., Li, Q., Fan, J., & Wang, X. 2024. Research on Soil Erosion Based on Remote Sensing Technology: A Review. *Agriculture*, *15*(1), 18. https://doi.org/10.3390/agriculture15010018

Wischmeier, W. H., Johnson, C. B., & Cross, B. 1971. Soil Erodibility Nomograph For Farmland and Construction Sites. *Journal of Soil and Water Conservation*. Retrieved from https://www.semanticscholar.org/paper/SOIL-ERODIBILITY-NOMOGRAPH-FOR-FARMLAND-AND-SITES-Wischmeier-Johnson/fdfd16b4abe9050bd9021c4ab1db98bafa52b80a

Wischmeier, W. H., & Smith, D. D. 1978. *Predicting Rainfall Erosion Losses: A Guide to Conservation Planning*. Department of Agriculture, Science and Education Administration. Retrieved from https://hero.epa.gov/reference/624965/

Xiong, M., Leng, G., & Tang, Q. 2023. Global Analysis of the Cover-Management Factor for Soil Erosion Modeling. *Remote Sensing*, *15*(11), 2868. https://doi.org/10.3390/rs15112868

Yang, X. 2015. Digital mapping of RUSLE slope length and steepness factor across New South Wales, Australia. *Soil Research*, *53*(2), 216. https://doi.org/10.1071/SR14208

Yuan, C., & Fan, H. 2024. Response mechanism of black soil structure to compound erosion forces in sloping farmland, Northeast China. *Soil and Tillage Research*, *240*, 106103. https://doi.org/10.1016/j.still.2024.106103